Available online at www.sciencedirect.com
SCIENCE DIRECT®
Surface and Coatings Technology 177–178 (2004) 312–316
SURFACE & COATINGS TECHNOLOGY
www.elsevier.com/locate/surfcoat

Microstructure evaluation and strengthening mechanism of Ni–P–W alloy coatings

F.B. Wu, S.K. Tien, W.Y. Chen, J.G. Duh*

Department of Materials Science and Engineering, National Tsing Hua University, Hsinchu, Taiwan

Abstract

Ni–P–W alloy coatings were deposited onto AISI420 steel substrates by both RF magnetron sputtering and electroless plating techniques. The coating hardness was investigated through the microhardness testing with a Knoop indenter. The strengthening mechanism of the Ni–P–W coatings in both as-deposited and heat-treated states were described with respect to compositional distribution and microstructural evolutions. In the as-deposited state, all the coatings exhibited amorphous/nanocrystalline structure. After heat treatment, the amorphous phase of Ni–P–W coatings transformed into Ni_3P precipitates and Ni(W) solid solution. The coatings were strengthened by the precipitation of Ni–P compounds and dissolving of W in the crystallized Ni matrix. With the aid of microstructure, the strengthening mechanism for the Ni–P–W coatings were proposed. Quantitative analysis for the strengthening effect of the Ni–P–W coatings was performed based on the elemental concentrations, Ni–P compound precipitation and Ni(W) matrix ratio. The heat-treated $Ni_{76.7}P_{15.9}W_{7.4}$ coating showed the highest peak hardness of 17.5 GPa when the maximum W solution in the Ni matrix was achieved.

Keywords: Ni–P-based ternary coating; RF magnetron sputtering; Electroless plating; Microhardness; Strengthening

1. Introduction

Nickel–phosphorous films are one of the well-known protective coating and widely adopted in versatile industrial applications owing to its merits in mechanical and chemical properties, such as uniform thickness, high hardness, corrosion and wear resistance [1–4]. Ni–P coating can be fabricated by various techniques including electroplating [5], electroless deposition [1–4], sputtering [6–9], etc. The as-deposited Ni–P coating is an amorphous or nanocrystalline Ni matrix supersaturated with P, and under appropriate thermal history, it can be hardened by the precipitation of nickel–phosphide compounds, such as Ni_3P, Ni_5P_2 and $Ni_{12}P_5$ [10–12], in the crystalline Ni matrix. This feature makes the Ni–P coating a suitable material for the application as a protective layer for injection or press molding dies. However, after excessive annealing or higher temperature usage the hardness of Ni–P films is degraded due to coarsening and grain growth of Ni_3P and Ni matrix [13]. The increase of the phase transformation temperature and the enhancement on coating hardness are thus critical to assure that the Ni–P deposit retains sufficient or even superior strength at elevated temperatures.

Encouraging results in optimizing characteristics of the Ni–P system by the introduction of a third element to form a ternary Ni–P-based alloy coating have been recently proposed, including Ni–Cu–P [14,15], Ni–W–P [10,16,17], Ni–Re–P [18], and Ni–Zn–P [19]. Thermal stability and surface hardness were improved by electroless Ni–Cu–P platings [7], as compared to Ni–P coating. An even superior improvement in surface hardness and phase transformation temperature was carried out by the incorporation of W instead of Cu into the Ni–P coating [8,17]. It is believed that W, which exhibits a relatively high hardness and a high melting point of 3410 °C, retards the Ni_3P precipitation and Ni crystallization, and thus promotes the mechanical and thermal properties of the Ni–P–W coatings. However, the detailed microstructure evolution and the strengthening mechanism for ternary Ni–P–W coatings are not yet fully understood. In the present study, intensive studies on microstructure evaluation of the Ni–P–W alloy coating were performed. The strengthening mechanisms of the Ni–P–W coating system fabricated by both electroless plating and magnetron sputtering techniques

*Corresponding author. Fax: +886-3-5712686.
E-mail address: jgd@mse.nthu.edu.tw (J.G. Duh).

0257-8972/04/$ - see front matter © 2003 Elsevier B.V. All rights reserved.
doi:10.1016/j.surfcoat.2003.09.010

Table 1
Composition and peak hardness of various Ni–P and Ni–P–W coatings after heat treatments

Deposition technique	Concentration (at.%)			Peak hardness (GPa)
	Ni	P	W	
Electroless	74.5	25.5	–	12.1 ± 0.9
Electroless	78.4	18.3	3.3	16.0 ± 1.0
Sputtering	80.0	15.3	4.7	15.7 ± 1.0
Sputtering	76.7	15.9	7.4	17.5 ± 1.5

was proposed according to microstructure features. Quantitative analysis on Ni_3P precipitation and Ni(W) matrix phases was conducted to correlate the hardness of the ternary Ni–P–W coating with the associated microstructure.

2. Experimental details

AISI 420 tool steel, which exhibited various merits including sufficient mechanical strength, good machinability, and cost effectiveness was chosen as substrate material. The binary Ni–P and ternary Ni–P–W coatings were deposited by both electroless plating and magnetron sputtering techniques. The electroless plating baths for Ni–P and Ni–P–W contained nickel sulfate (0.075 M), sodium citrate (0.4 M), sodium hypophosphite (0.1 M), and sodium tungstate (0.2 M) (used only in Ni–P–W deposition process). The pH value during electroless plating was controlled at 9.0 by the 50 vol.% NH_4OH and 20 vol.% H_2SO_4. The bath temperature and plating time were 93 ± 1 °C and 2 h, respectively. The sputtered Ni–P–W coatings were fabricated with a dual-gun system equipped with two identical sputtering guns. A 300 μm electroless $Ni_{79.5}P_{20.5}$ coated Cu disk and a pure W disk both of 76.2 mm in diameter were loaded in the vacuum chamber as sputtering sources. The input power on the Ni–P/Cu target was 200 W, while that for the W target was controlled at 35 and 50 W. The working pressure and target-to-substrate distance were 4.0×10^{-1} Pa and 60 mm, respectively. The deposition time of the sputtered Ni–P–W coating was controlled at 4 h. Details in experimental procedures for fabrication of the electroless and sputtered Ni–P–W coatings could be referred in preliminary studies by Tsai et al. [17] and Wu et al. [8], respectively. The as-deposited Ni–P and Ni–P–W coatings were heat-treated at temperatures of 350–600 °C for 4 h in a nitrogen purged chamber, and were then furnace-cooled to room temperature.

The compositions of the coatings were evaluated with an electron probe microanalyzer (EPMA, JXA-8800M, JEOL, Japan) with ZAF (atomic number, absorption and fluorescence) correction methods [20]. Phase identification was performed with an X-ray diffractometer (Dmmax, Rikagu, Tokyo, Japan). A high-resolution transmission electron microscope (HRTEM, JEM-2010, JEOL, Japan) was employed to examine the detailed microstructure of the Ni–P–W coatings. Structural analysis was performed by selected area electron diffraction (SAED) method. The microhardness of the coatings was measured with a microhardness tester (MHT-4, Anton Paar, Austria) equipped with a Knoop indenter. The peak hardness of each coating, as listed in Table 1, was defined as the maximum hardness for every coating under series heat treatment from 350 to 600 °C.

3. Results and discussion

3.1. Material systems and microstructure

Both electroless and sputtering techniques were employed to fabricate the Ni–P–W coating. The chemical composition of Ni–P and Ni–P–W coatings are according to Table 1, electroless $Ni_{74.5}P_{25.5}$, electroless $Ni_{78.4}P_{18.3}W_{3.3}$, sputtered $Ni_{80.0}P_{15.3}W_{4.7}$, and sputtered $Ni_{76.7}P_{15.9}W_{7.4}$ coatings. The film thicknesses of the electroless and sputtered coatings were 6 μm and 3 μm, respectively.

Microstructure of the as-deposited electroless Ni–P was reported to be nanocrystalline or even amorphous according to the P contents in the binary Ni–P coatings [21]. X-Ray diffraction patterns of the as-deposited Ni–P and Ni–P–W coatings fabricated by both electroless and sputtering techniques are shown in Fig. 1. All the patterns showed the Fe(110) peak of the steel substrate and a broadened peak with a width approximately 40–50°. It is believed that the as-deposited electroless and sputtered Ni–P–W coatings have an amorphous or nanocrystalline microstructure like the as-deposited electroless Ni–P deposit.

Fig. 2a,b represent the DSC curves of the electroless $Ni_{78.4}P_{18.3}W_{3.3}$ and sputtered $Ni_{76.7}P_{15.9}W_{7.4}$ coatings,

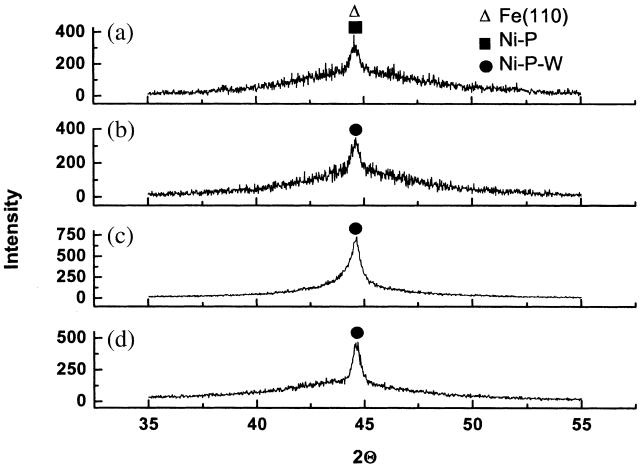

Fig. 1. X-Ray diffraction patterns of the as-deposited (a) electroless $Ni_{74.5}P_{25.5}$; (b) electroless $Ni_{78.4}P_{18.3}W_{3.3}$; (c) sputtered $Ni_{80.0}P_{15.3}W_{4.7}$; and d) sputtered $Ni_{76.7}P_{15.9}W_{7.4}$ coatings.

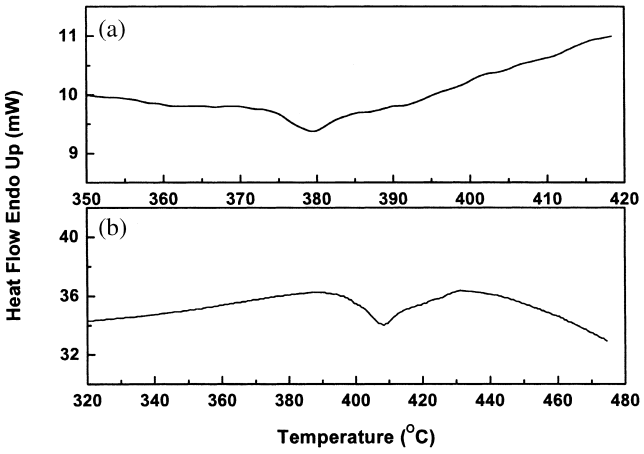

Fig. 2. DSC curves of the electroless $Ni_{78.4}.P_{18.3}W_{3.3}$ and sputtered $Ni_{76.7}P_{15.9}W_{7.4}$ coatings.

respectively. The exothermic peak of the electroless $Ni_{78.4}P_{18.3}W_{3.3}$ deposit was observed at approximately 380 °C, while that of the sputtered $Ni_{76.7}P_{15.9}W_{7.4}$ coating was at 410 °C. Generally, the crystallization temperature for binary Ni–P coatings is 350 °C. With higher annealing temperatures or elongated heat-treating time, the amorphous Ni–P would transform into Ni_3P and Ni crystalline phases. The introduction of W into the Ni–P system postponed the phase transformation of Ni_3P precipitation and Ni crystallization. The higher the co-deposition quantity of W into the Ni–P system is, the higher is the increase of the phase transformation temperature. Thus, the sputtered $Ni_{76.7}P_{15.9}W_{7.4}$ coating exhibited a crystallization temperature of 410 °C.

Phase transformation through thermal history for Ni–P–W coatings was analyzed by TEM technique. The diffraction pattern and TEM plane image of the $Ni_{76.7}P_{15.9}W_{7.4}$ coating heat-treated at 500 °C for 4 h are shown in Fig. 3. The crystallization process for the Ni–P–W coating after heat treatment was finished according to the distinct diffraction spots. The narrow diffraction rings indicate that the amorphous/nanocrystalline Ni–P–W transformed into polycrystalline Ni_3P and Ni phases. The phase transformation could also be evidenced by the randomly distributed Ni crystallites with a size of 10–30 nm as shown in Fig. 3b. From the first ring of the diffraction pattern, the lattice spacing was calculated to be 0.2085 nm, which was larger than that of the standard Ni(111) at 0.2034 nm. It is argued that W, which has a larger atomic size than Ni dissolute into the Ni matrix and enlarges the lattice. Similar results could be referred in literatures. Tsai and coworkers [17] investigated the crystallization behavior of electroless Ni–P–W deposits after heat treatment by X-ray diffraction technique. It was concluded that the co-plated W formed a Ni–W solid solution with Ni matrix and thus the 2θ angle of Ni(111) diffraction peak shifted to lower degrees approximately 44.5 °C. Koiwa et al. [22] provided a survey of crystallization phenomenon of the Ni–P–W systems. After heat treatment, the Ni–P–W alloy transformed into Ni_3P and Ni(W) phases. In the present case, the Ni–P–W coating transformed into Ni_3P and Ni(W) phases with an amorphous/nanocrystalline microstructure.

3.2. Strengthening mechanism

Through an adequate annealing process, the as-deposited Ni–P alloy coating would transform to Ni_3P and Ni crystalline phases, which was the final products of the Ni–P alloy [11,23]. Binary Ni–P alloy could be hardened by Ni_3P precipitation within the Ni crystalline matrix. Table 1 indicates the peak hardness of various Ni–P–W coatings, under series of heat treatments at temperatures ranging from 350 to 600 °C for 4 h. As listed in Table 1, the heat-treated $Ni_{74.5}P_{25.5}$ coating showed a higher hardness, 12.1 GPa, than that of the as-deposited Ni–P coating, 6.2 GPa [17], due to the phase transformation. For the W incorporated Ni–P coatings, hardening by W solid solution hardening in Ni matrix was considered as another strengthening mechanism as described in the previous section. Further

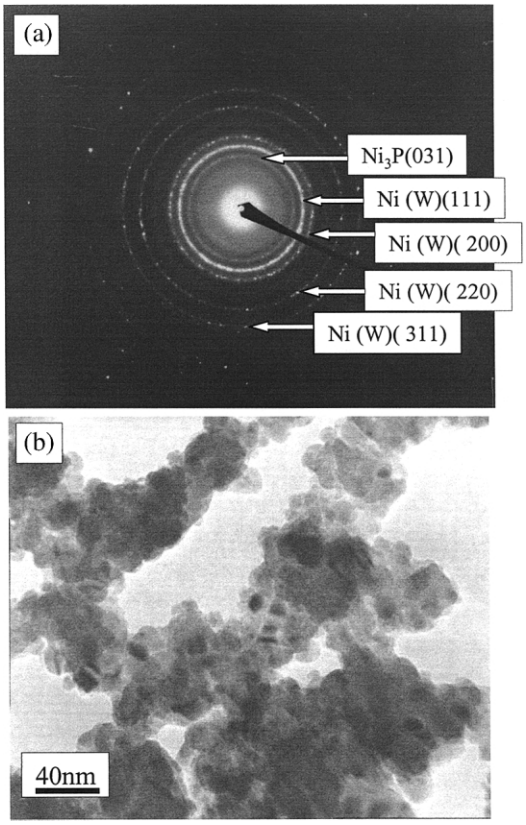

Fig. 3. (a) Electron diffraction pattern and (b) TEM micrograph of the $Ni_{76.7}P_{15.9}W_{7.4}$ coating heat-treated at 500 °C for 4 h.

enhancement in hardness was found for the heat-treated Ni–P–W coatings (>16 GPa) as compared to that of the heat-treated Ni–P (approx. 12.4 GPa).

To have a quantitative description of the strengthening effect in Ni–P and Ni–P–W coating systems, the phase transformation phenomenon is described as following equations:

$$\mathrm{Ni-P(as\text{-}deposited)} \xrightarrow{\text{heat-treatment}} \mathrm{Ni_3P + Ni} \quad (1)$$

$$\mathrm{Ni-P-W(as\text{-}deposited)} \xrightarrow{\text{heat-treatment}} \mathrm{Ni_3P + Ni(W)} \quad (2)$$

These two equations represent only the final products Ni_3P, Ni and/or Ni(W), metastable phases, including Ni_5P_2, $Ni_{15}P_2$, etc. are not taken into consideration.

According to the phase diagram [5], P exhibited negligible dissolution in the Ni matrix. Thus, P in the Ni–P–W coating was presumably contributed to the formation of Ni_3P phase under adequate heat treatment. Furthermore, it was demonstrated through electron diffraction technique that the co-deposited W element dissolved in the Ni matrix to form a Ni(W) solid solution after annealing. Meanwhile, no W or W related compounds were observed in the diffraction patterns. The co-plated W acts as a solutioning element in the Ni crystalline phase. The phase transformation phenomenon of Ni–P and Ni–P–W coating after heat treatment could be constructed as Eqs. (1) and (2) on the basis of the above-mentioned experimental findings and physical evidences.

3.3. Quantitative analysis on strengthening factors

From Eq. (2), the phase transformation function could be modified with constants:

$$\mathrm{Ni}_a\mathrm{P}_b\mathrm{W}_c \xrightarrow{\text{annealing}} b\mathrm{Ni_3P} + (a-3b)\mathrm{Ni(W)} \quad (3)$$

where *a*, *b* and *c* are the atomic concentration of Ni, P and W, as indicated in Table 1.

To investigate the influences of Ni_3P, Ni(W) matrix and W/Ni(W) matrix ratio on strengthening of the Ni–P–W coating systems, quantitative analysis was performed with respect to W contents in the ternary coatings with the aid of Eq. (3), as indicated in Fig. 4. The molar ratios of Ni(W) matrix and Ni_3P precipitation against W content were plotted in Fig. 4b,c, respectively. It is interesting to find that the amounts of Ni(W) and Ni_3P phases remained unchanged for the sputtered films in spite of the addition of W to the coating. However, the fraction of the Ni(W) matrix of the electroless coating increased from 75 to 86, the Ni_3P decreased rapidly from 25 to 14 as W was added from 0 to 3.5 at.% in the Ni–P–W coating. It appears that W to

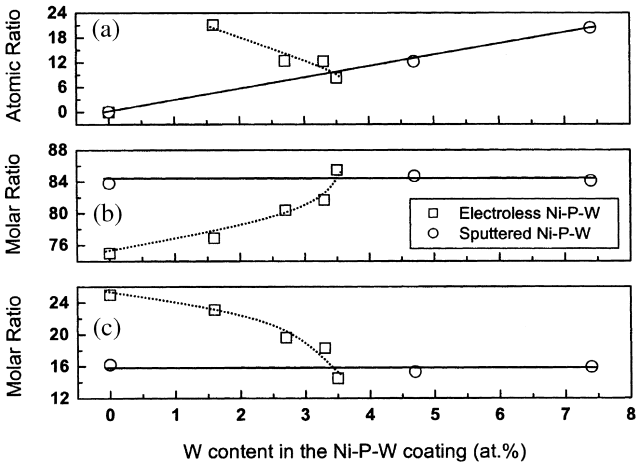

Fig. 4. Quantitative analysis of (a) W/Ni(W) ratio; (b) Ni(W) matrix; and (c) Ni_3P, in various ternary electroless and sputtered Ni–P–W coatings after heat treatments.

Ni(W) ratio in the sputtered films increased linearly when the W was increased. On the contrary, W to Ni(W) ratio in the electroless coating reduced from 20 to 6 as the W content increased from 1.6 to 3.5.

The precipitation of Ni_3P phase was one of the major factors in hardening the Ni–P coating. For the electroless Ni–P–W coatings, Ni(W) solid solution could provide another strengthening factor as described previously. It should be noticed that the W/Ni(W) ratio represented the degree of solid solutioning of W in the Ni(W) matrix, implying the degree of solid solution hardening. Since the W element was classified as a hard material, the higher the amount of W in the Ni(W) alloy is, the harder is the solid solution Ni(W) phase. In the present case, though the hard Ni(W) phase was increased with the increasing of W, the quantity of Ni_3P phase decreased to almost half of the amount (from 25 to 14). Moreover, the W/Ni(W) ratio dropped enormously from 20 to 6 as W increased from 1.6 to 3.5, indicating an anti-strengthening effect on the Ni(W) matrix. As a result, increasing the W content in the electroless Ni–P–W coating could not induce a higher content of the Ni_3P phase and higher Ni(W) solutioning degree to increase the coating hardness after heat treatment.

The situation for the sputtered Ni–P–W coatings was different from that of the electroless ones. The quantities of Ni_3P and Ni(W) phases were indepedent of W content in the ternary Ni–P–W coatings. Meanwhile, the solutioning degree, W/Ni(W) ratio was increased with W content. Consequently, the hardness of Ni(W) increased and this in turn promoted the Ni–P–W coating hardness.

The peak hardness values of various coatings after heat treatment, as summarized in Table 1, provide another evidence for the strengthening mechanism of Ni_3P and Ni(W) phases. For ternary Ni–P–W coatings, the introduction of W to form a Ni(W) phase in the

heat-treated Ni–P–W successfully increased the hardness as compared to the binary Ni–P coating. The peak hardnesses of the $Ni_{78.4}P_{18.3}W_{3.3}$ and $Ni_{80.0}P_{15.3}W_{4.7}$ deposits were more or less at the same level of 16 GPa, although the latter coating exhibited a higher W content. This was because the molar ratios of Ni(W) and Ni_3P phases, as indicated in Fig. 4b,c of each coating were close to each other, 84 and 16, respectively. In addition, these two coatings had identical degree of W/Ni(W) ratio approximately 12, as plotted in Fig. 4a. The influence of the W incorporation degree in Ni(W) phase on coating hardness could be further demonstrated with the sputtered $Ni_{80.0}$,$P_{15.3}$,$W_{4.7}$ and $Ni_{76.7}P_{15.9}W_{7.4}$ coatings. As indicated in Table 1, the $Ni_{76.7}P_{15.9}W_{7.4}$ deposit exhibited a peak hardness of approximately 18 GPa, which was higher than that of the $Ni_{80.0}P_{15.3}W_{4.7}$ coating, 16 GPa. The Ni(W) and Ni_3P molar ratios of both coatings were approximately 84 and 16, respectively. However, the W/N(W) value of the $Ni_{76.7}P_{15.9}W_{7.4}$ deposit was much higher than that of the $Ni_{80.0}P_{15.3}W_{4.7}$ coating. As a consequence, the $Ni_{76.7}P_{15.9}W_{7.4}$ deposit with higher degree of W/Ni(W) solid solution strengthening showed a harder coating characteristic as compared to the electroeiss $Ni_{78\ 4}P_{18.3}W_{3.3}$ and sputtered $Ni_{80.0}P_{15.3}W_{4.7}$ coatings.

4. Conclusion

The Ni–P–W coating systems with W content ranged from 0 to 7.4 at.% were investigated. The as-deposited Ni–P and Ni–P–W coatings both fabricated by electroless and sputtering techniques exhibited an amorphous/nanocrystalline feature. DSC results indicated that the introduction of W effectively shifted the phase transformation temperature from 350 °C for binary Ni–P deposit to 410 °C for $Ni_{76.7}P_{15.9}W_{7.4}$ coatings. After 500 °C, heat treatment for 4 h, the Ni_3P precipitation and Ni(W) crystalline phases could be identified for the $Ni_{76.7}P_{15.9}W_{7.4}$ coating. The lattice spacing expansion of Ni(111) from 0.2034 to 0.2085 nm was attributed to the W dissolution in the Ni matrix to form a Ni(W) alloy.

The strengthening mechanism was proposed on the basis of microstructural features, physical evidences and hardness values. The Ni–P–W coatings were hardened not only by the precipitation of Ni_3P precipitation but also by the Ni(W) solid solution matrix after heat treatment. Quantitative analysis was performed with the aid of a phase transformation function. The quantities of Ni_3P and Ni(W) in the coating and the W/Ni(W) ratio were calculated and successfully employed to describe the hardening effect. The peak hardness of the electroless Ni–P–W coating after heat treatment was not enhanced by the increase of W content, since the Ni_3P phase and the W/Ni(W) ratio was decreased. On the contrary, with the increase of W in the sputtered Ni–P–W deposits, the Ni_3P and Ni(W) phases remained unchanged and the W/Ni(W) ratio increased from approximately 12 to 20, resulting in the enhancement in the coating hardness from 16.0 to 17.5 GPa.

Acknowledgments

The support of this work from National Science Council under the contracts No.NSC90-2216-E-007-070 and NSC91-2216-E-007-03 5 is appreciated.

References

[1] G.O. Mallory, J.B. Hajdu, Electroless Plating: Fundamentals and Applications, America Electroplaters and Surface Finishers Society, Orlando, FL, 1990, p. 1, Chapter 4.
[2] J.A. Sue, T.P. Chang, Surf. Coat. Technol. 76–77 (1995) 61.
[3] L.F. Spencer, Met. Finish. (1974) 35.
[4] Y. Chiba, T. Ornura, H. Ichimura, J. Mater. Res. 8 (1993) 1109.
[5] W.H. Safranek, The Properties of Electrodeposited Metals and Alloys, 2nd ed, America Electroplaters and Surface Finishers Society, Orlando, FL, 1986, p. 345.
[6] J.S. Yoon, H.J. Doerr, C.V. Deshpandey, R.F. Bunshah, J. Electrochem. Soc. 136 (1989) 3513.
[7] Y.C. Chang, J.G. Duh, Y.I. Chen, Surf. Coat. Technol. 139 (2001) 233.
[8] F.B. Wu, Y.I. Chen, P.J. Peng, Y.Y. Tsai, J.G. Duh, Surf. Coat. Technol. 150 (2002) 232.
[9] F.B. Wu, S.K. Tien, J.G. Duh, J.H. Wang, Surf. Coat. Technol. 166 (2003) 60.
[10] P. Nash, Phase Diagrams of Binary Nickel Alloys, ASM International, June 1991, p. 235.
[11] P.S. Kumar, P.K. Nair, J. Mater. Process. Technol. 56 (1996) 511.
[12] F.B. Wu, J.J. Li, J.G. Duh, Thin Solid Films 377–378 (2000) 354.
[13] J.K. Dennis, T.E. Such, Nickel and Chromium Plating, 2nd ed, Butterworths and Co Ltd, London, 1986, p. 276.
[14] Y.W. Wang, C.G. Xiao, Z.G. Deng, Plat. Surf. Finish. (March 1992) 57.
[15] S. Armyanov, O. Steenhaut, N. Krasteva, J. Geogeorgieva, J.-L. Delplancke, R. Winand, et al., J. Electrochem. Soc. 143 (1996) 3692.
[16] B.W. Zhang, W.Y. Hu, Q.L. Zhang, X.Y. Qu, Mater. Charact. 37 (1996) 119.
[17] Y.Y. Tsai, F.B. Wu, Y.I. Chen, P.J. Peng, J.G. Duh, S.Y. Tsai, Surf. Coat. Technol. 146–147 (2001) 502.
[18] D. Mencer, J. Alloys Compd. 306 (2000) 158.
[19] M. Boanani, F. Cherkaoui, R. Fratesi, G. Roventi, G. Barucca, J. Appl. Electrochem. 29 (1999) 637.
[20] J.I. Goldstein, D.E. Newbury, P. Echlin, D.C. Joy, C. Fiori, E. Lifshin, Scanning Electron Microscopy and X-ray Microanalysis, Plenum Press, 1981.
[21] K.L. Linand, P.J. Lai, J. Electrochem. Soc. 136 (1989) 3803.
[22] I. Koiwa, M. Usuda, T. Osaka, J. Electrochem. Soc. 135 (1988) 1222.
[23] P.R. Krishnamoorthy, B.H. Narayana, T.V. Ramakrishna, M.S. Kumar, Met. Finish. (November 1992) 13.